HANS J. BERNATH*
University of Washington
Seattle, Wash. 98195

Radiometric Calibration of a Multi-Spectral Aerial Camera

The use of an aerial camera as a spectroradiometer requires a careful calibration of the lenses, filters, shutter and film as well as the understanding of the intervening atmosphere.

ABSTRACT: *Under a USGS-EROS grant the University of Washington has acquired an International Imaging System (I²S) Mark I multispectral camera. A preliminary examination of the photographs showed image quality variations of such an extent that the data were of questionable value for accurate tonal analysis. As a consequence it was decided to re-examine the imaging system and the parameters affecting image quality. After calibration and with the aid of an idealized atmospheric model, the reliability of the radiometric measurements was considerably increased. A first test showed that an accuracy in the neighborhood of ± 3 percent absolute ground reflection could be achieved by the calibrated system.*

IN THE LAST few years multispectral aerial photography has enjoyed a rapidly increasing interest and the group of users grew accordingly. But from contacts with many of the non-research oriented buyers of multispectral cameras and supplementary equipment the author concludes that the obtained results are often not as satisfying as expected, and are sometimes rather disappointing. Difficulties in obtaining good color renditions and repeatable results are very common. The reason for the unexpected complications is the relatively large number of parameters affecting final image quality as well as the greater sensibility to misregistration compared with the more familiar panchromatic photography. Yost[9] writes in one of his early articles about this problem:

> "To be certain that the density difference is in fact caused by the difference in spectral reflectance of the object on the ground it is essential that (1) the camera system be spectrometrically calibrated, (2) the spectral distribution of the illumination be known, (3) the spectral bands covered by each photograph be correctly chosen and (4) the photographic processing be precisely controlled."

The following pages describe a relatively simple calibration technique to satisfy the requirements as stated above. As environmental effects have a major impact on radiometric measurements, the term calibration is used in a somewhat broader sense than usual. Calibration in this context is defined as measurement of the camera characteristics and the relevant environmental parameters.

The experiments were conducted between January and June, 1972. All the measurements relate to the International Imaging System (I²S) Mark I camera purchased by the University of Washington under a USGS-EROS contract.

DENSITOMETRY

The key problem of any photoradiometric measurement is to find the relationship between film density and object reflectance. Let us therefore briefly review the basic radiometric equations on which our calculations will be based.[2] Figure 1 shows the radiant energy as it flows through the I²S sensor system. The solar energy on its path through the atmosphere is attenuated by

* The author received the Bausch & Lomb Photogrammetric Award for this, the best paper on photogrammetry by a college (graduate) student, at the Annual Convention of the American Society of Photogrammetry, Washington, D.C., March 1973.

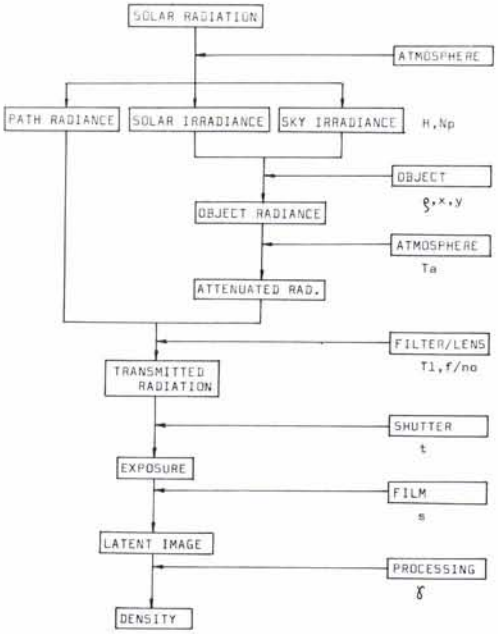

FIG. 1. Scheme of an aerial photographic system. The left-hand side shows the transformation of light energy into image density. The intervening camera and environmental parameters are listed on the right side.

absorption and scattering. The downward scattered part of the light is usually called skylight. The upward scattered part makes up what is named path radiance. Depending on atmospheric conditions and solar altitude, a variable amount of unscattered solar radiation reaches the earth's surface. Thus an object is illuminated by direct solar and sky irradiance.

On its path from the object to the camera the radiant flux is again attenuated. The lens finally collects the remaining ground reflected energy plus the upward scattered path radiance. The total radiance N_t as seen by the camera becomes therefore:

$$N_t = \frac{1}{\pi}(\rho T_a H + N_p) \qquad (1)$$

where ρ is surface albedo, T_a is the atmospheric transmittance, H is the solar plus sky irradiance and N_p is the path radiance. The collected light is imaged onto the image plane. The irradiance of the film H' becomes:

$$H' = (\rho H T_a + N_p)\cos^4\phi/(f/no)^2 \qquad (2)$$

where f/no is the relative aperture and φ is the nadir scan angle. This formula is only correct for a perfect lens system with no fall-off. In reality the theoretical $\cos^4$-function will seldom be encountered. Equation 2 should rather be written as:

$$H' = (\rho H T_a + N_p)T_1/(f/no)^2 \qquad (3)$$

where T_1 is the lens transmittance. The exposure is now defined as the product of duration of shutter opening t and image irradiance H'. The film response to exposure and development is finally represented by a characteristic curve whose straight-line portion is approximated by:

$$D = Do + \gamma \log\left[\frac{(\rho H T_a + N_p)tT_1 \cdot s}{(f/no)^2}\right] \qquad (4)$$

where s is the film sensitivity depending on wavelength.

Before entering into more detailed discussion of the different parameters, let us analyze Equation 4 for a moment. Two groups of parameters can be distinguished: (1) camera parameters (γ, T_1, t, s, f/no) and (2) environmental parameters (H, N_p, T_a, ρ)

The camera parameters are expected to remain constant for a given experiment and probably for a whole series of experiments. Thus, their impact on photographic density can be predicted and expressed by a mathematical function. In conventional terminology the measurements of these parameters could be called radiometric calibration. The nature of the environmental parameters is different insofar as they change rapidly and are difficult to forecast. If they stay constant during one overflight they will most probably vary between different surveys. Their control is very often neglected, which is one major cause for inability to reproduce results. Thus, it must be emphasized that the radiometric calibration of a multispectral camera must include some detailed instructions for the reduction and compensation for environmental effects.

CAMERA PARAMETERS

The main components of a camera causing variations in image density are: the shutter (exposure time), the lens system (transmission), and the film (sensitivity and processing). Their characteristics vary for different camera designs and the test procedures must be adapted to the specific type.

EXPOSURE TIME

The shutter of the I²S camera is of the focal-plane type. The camera dial shows an exposure time range of 1/150 to 1/350. As

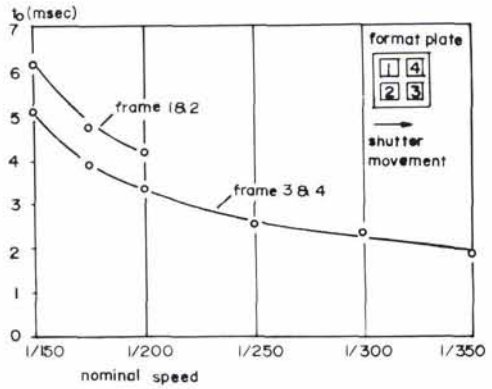

FIG. 2. Results of the shutter test. The measured duration of shutter opening t_o is displayed *vs.* time setting on the camera dial. The measurements were taken in the center of frames 2 and 3. The exposure times differ by approx. 25 percent.

only the extreme values of the scale are marked, intermediate settings have to be interpolated. The manufacturer gives no indication how the interpolation has to be performed. Thus, a linear relationship was assumed between lever rotation and speed.

A shutter test was designed to provide a measure of expected reliability. After removal of the lens board a condensed light source (sunlight) was projected through the shutter onto a photo diode. The diode's signal was fed to an oscilloscope and displayed *vs.* time. Figure 2 shows the results. Comparing the values for frame 2 and 3 it can be seen that the exposure times differ by more than 20 percent. The difference is caused by shutter acceleration. The standard deviation of measurements on a single frame was as high as 7 percent. The two numbers together suggest strongly that the movement of the shutter is very irregular and almost impossible to predict with a better accuracy than 10 percent.

The efficiency Ef of the focal plane shutter is only a function of camera geometry[3] and can be written as:

$$Ef = 100\ w/[w + d/(f/no)] \tag{5}$$

where w is the slit width of shutter, d is the distance between shutter plane and focal plane and f/no is the calibrated relative aperture.

Figure 3 shows a family of curves generated from Figure 2 and Equation 5. The values given by the graph are valid for Frames 3 and 4. Approximate exposure times for Frames 1 and 2 are found by multiplying the corresponding numbers by 1.2.

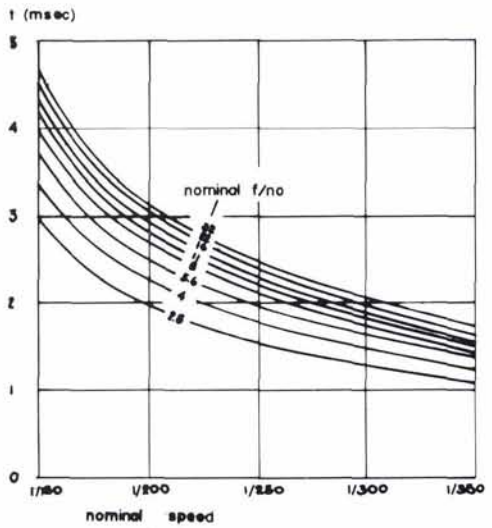

FIG. 3. Effective exposure times t as a function of lens aperture (nominal f/no) and exposure time setting on the camera dial. The curves were obtained by a combination of Figure 2 and Equation 5. The graph gives the values for lenses 3 and 4.

LENS TRANSMISSION

The four lens systems consist basically of three parts (Figure 4):

- —before the lens interference filter (IR blocking) except for band four
- —Brooks-Schneider Kreuznach 100mm f/2.8 Xenotar lens
- —Between-the-lens filter (Wratten passing for desired spectral band)

As the focal lengths of the lenses are theoretically selected to be approximately

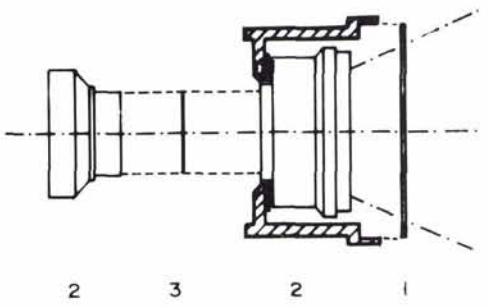

FIG. 4. Section through the lens system. The parts are: (1) before-the-lens interference filter (IR-blocking), (2) Brooks Schneider Kreuznach 100 mm, f/2.8 Xenotar lens, and (3) between-the-lens filter (Wratten passing for desired spectral band).

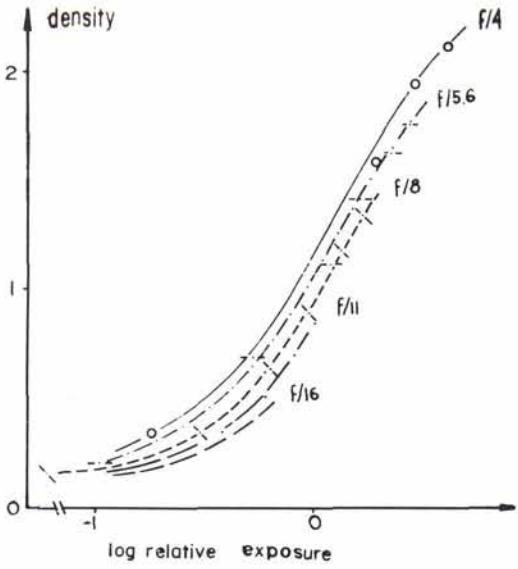

FIG. 5. The graph represents five photographs of a gray step target of known reflectances taken under constant illumination. Theoretically, the five curves should match perfectly. The shift is due to the change in light energy absorption and reflection by the actual glass for different shutter settings. (Measurements for lens 1).

matched to the assigned bands, the filter-lens combination should not be interchanged. The given combination can therefore be considered as fixed. For this reason the transmission characteristics were tested on the filter-lens assembly as a whole.

The amount of light energy transmitted depends strongly on a number of geometric as well as radiometric parameters. The most readily understandable variation in exposure is obtained by different lens apertures as indicated by the change in f/no. However, as an indication of the light-passing power, the f/no ignores the change in light energy absorption and reflection by the actual glass for different lens settings. This effect is clearly demonstrated by Figure 5. The graph represents a sequence of photographs of a gray step target of known reflectances taken under constant illumination. The relative exposure E was calculated after the following formula:

$$E = k\rho/(f/no)^2 \tag{6}$$

where k is a constant and ρ is surface albedo.

Plotting $log\ E$ against the measured density, a series of slightly offset curves of constant γ are generated. The shift in relative exposure shows that the changing transmission had not been taken into account.[6] Consequently, the relative exposures were recomputed after the modified formula:

$$E = k\rho/(T/no)^2 \tag{7}$$

where $(T/no) = (f/no)/\sqrt{\tau}$ *and* τ is the relative center transmission. The T-numbers for the blue band are listed in Table 1.

TABLE 1. T/no FOR LENS 1

f/no	T/no
2.8	3.8
4	5.3
5.6	8.0
8	11.6
11	16.2
16	22.1

The dependence of the lens transmission upon angle of incidence is a classical problem of photography. In a simple lens system the irradiance of the image plane is proportional to the $\cos^4$ of the nadir scan angle. However, most modern lenses are designed with variations from this fundamental physical law.[1] Furthermore, the fall-off characteristics are not expected to be the same for different lens openings. This fact is of special importance to multispectral photography as different lens openings are used to compensate for the largely different amounts of object reflected energy in the four bands (Figure 6). The test described below was designed to meas-

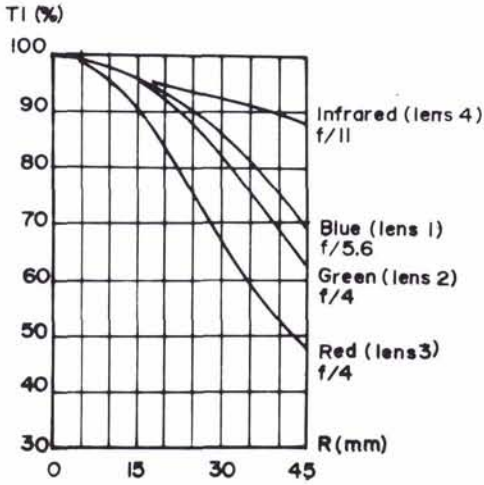

FIG. 6. Light intensity fall-off in the image plane. The curves show the fall-off characteristics for the four lenses. The f/no correspond to the standard settings as used for the present series of experiments.

ure the specific fall off curves for the four lens-filter assemblies.

A series of 2 × 2-foot color panels, each painted blue, green, red and yellow were aligned across the principal point of the frame. The experiment requires targets of Lambertian surfaces. A photometric reflectance measurement showed that this was not exactly the case. It was also observed that the directional dependence did not follow the same pattern for all four bands. A more critical problem was the geometry of the lay-out. It is very important that the focal plane of the camera is parallel to the plane of the displayed targets. If this is not the case the density measurement will be distorted. After development, the target images were measured with a Joyce-Loebl microdensity scanner. To relate film density to transmission, a gray step target had been photographed together with the calibration panels. This set up is needed for the determination of the *D-log E* curve from which the relative exposure values were interpolated. The *lens transmission* T_l thus becomes:

$$T_l = T_{lr}/T_{lc} = E_r/E_c \qquad (8)$$

where E_c is the relative exposure in the center of the lens and E_r is the relative exposure at a distance r from the center.

Spectral transmission curves of the four lenses were obtained on a conventional double-beam photospectrometer. To eliminate any spectral distortion due to the before-the-lens interference filter, the test objective has to be aligned to the light path of the instrument. Curves for the filter transmission alone, obtained from repeated measurements with the filter at different angles to the light beam, showed a spectral shift of the magnitude of 10 nm. Fortunately, the shift is not large enough to affect the relatively broad spectral passband used.

FILM AND PROCESSING

Repeatability or reliability of multispectral photography is strongly limited by the control of the developing process. It is evident that tone variations caused by random variations in processing disturb the reciprocity between film density and exposure. To overcome these problems we may decide upon two principal approaches: either (1) the development conditions are so accurately controlled and kept constant in order to hold variations smaller than a certain threshold value, or (2) the variations are accepted and a method is found to measure and compensate for them. Certainly the first approach is the more satisfying but the second method may be the only possible one if precision processing is not available.

The author found himself in the latter situation. It was therefore decided to equip the camera with a light source of constant exposure. In the center of the format plate a light-emitting diode (LED) was installed and connected to the power pulse of the intervalometer. At the instant of shutter release the LED turns on for 40 msec. The light produces a spot of constant density for constant development, and thus a variation in development is revealed by a change in spot density. The intensity of the LED was adjusted so that its maximum exposure fell on the straight-line portion of the *D-logE* curve (Figure 7), which makes the relationship between density and γ a linear one (Table 2). The consistency of the density spot and consequently the accuracy of the control is given by the consistency of the exposure. The main limitation comes from the variations in timing which was measured to be ± 3 percent.

ATMOSPHERIC EFFECTS

In the last few years an increasing number

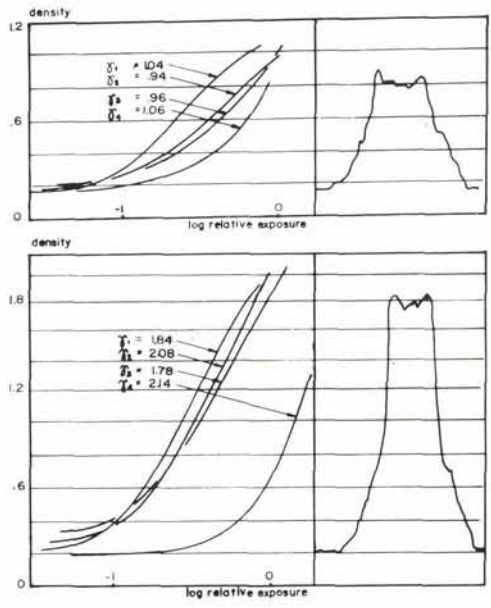

FIG. 7. Examples of *D-log E* curves and density spot traces. The two graphs were obtained by changing developing times. All experiments were conducted with Kodak Infrared Film 2424. (Subscripts: 1—blue, 2—green, 3—red, 4—infrared).

TABLE 2. SUMMARY OF STANDARD CAMERA PARAMETERS AS USED FOR THE PRESENT EXPERIMENTS. ($D°$ = DENSITY MEASURED IN THE CENTER OF THE IMAGE OF THE LIGHT-EMITTING DIODE, † = KODAK INFRARED FILM 2424)

		Blueband	*Greenband*	*Redband*	*IR-band*	σ
Nominal f/no	f/no	5.6	4	4	11	6%
Exposure Time	t	3.96 msec	5.70	4.75	3.03	2%
T-Number	T/no	8.00	5.3	5.3	16.2	5%
Radial Fall-Off Function	T_1	$\cos^4$	$\cos^5$	$\cos^7$	$\cos^2$	2%
Slope of D-log E Curve	γ	$.239 + .900D°$	$-.133 + 1.247D$	$.046 + 1.075D$	$.048 + 1.265D$	3%
Relative Film Filter Response	R‡	8.24	.955	7.95	6.66	
Spectral Pass Band	λ	385-460 nm	450-585 nm	590-740 nm	735-935 nm	

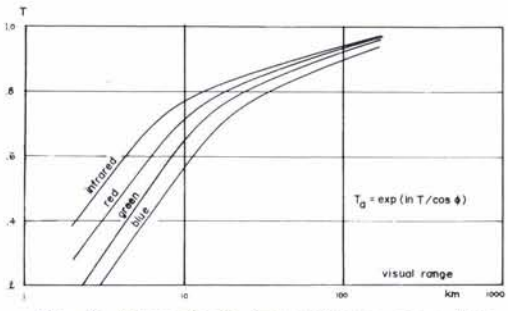

FIG. 8. Atmospheric transmittance as a function of visual range for a flying height of 3 km and a nadir scan angle of 0°. (Data compiled from Turner[7,8]).

of authors have stressed the need for better understanding of the atmospheric or environmental effects on aerial photography. Principally there have been two different approaches proposed for the solution to this problem. Turner[7,8] developed a mathematical model that allows for the determination of atmospheric transmission, path radiance and solar and sky irradiance. A more empirical technique was described by Piech.[5] He computes the same parameters, not by the aid of a radiative transfer model, but by comparative measurements on the photograph itself. The method applied by the author combines parts of the two and modifies them for the specific problem.

Before going into greater detail let us remember that any abstract description of the atmosphere must be a more or less rigorous simplification of the actual highly complex interactions. In other words, any mathematical model has its definite limitations. Simplicity may most probably mean a narrower range of validity. Or conversely the elimination of flight missions under extreme atmospheric conditions may permit the use of a simpler correction function. Thus, the problem can be significantly simplified by proper flight planning. Standards and minimum requirements should be established for the atmospheric conditions per se as well as for the sensor system. Parameters to be considered can be listed as:

Atmospheric Transparency
Time of Flights
Flight Direction (Azimuth)
Flying Height and Focal Length.

The atmospheric transmission is conveniently described by the visual range V[4]. Figure 8 shows the relationship as described by Turner.[7,8] The graph suggests the setting of a lower boundary of V at about 20 km

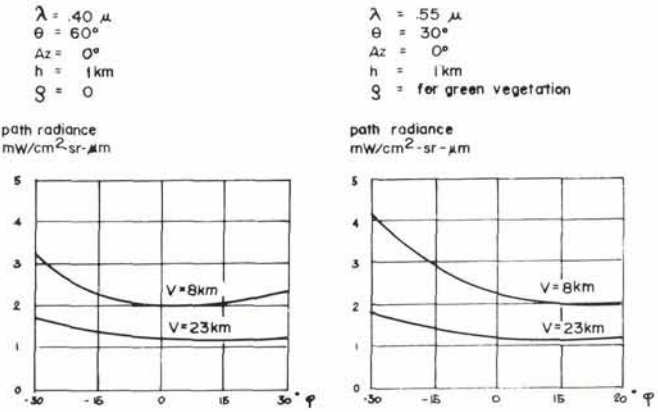

FIG. 9. Dependence of path radiance on nadir scan angle. The asymmetry is smaller for better visibility. The maximum scan angle of the tested camera is approx. 33°. (Data compiled from Turner[7,8]).

below which the atmospheric transmission becomes very sensitive to an error in estimation of the visual range. The exclusion of hazy conditions as defined by $V < 20$ *km* limits also the asymmetry of the path radiance (Figure 9). Keeping in mind that the back-scattered light can contribute a significant part to the total energy collected by the camera lens, it is conceivable that asymmetry will cause a remarkable tonal distortion. In limiting flight missions to better atmospheric conditions, however, the path radiance can be considered symmetric at least within a certain range of the nadir scan angle. This leads to the next parameter in the list, namely the lens or, more properly, the focal length. To eliminate extensive asymmetry superwide-angle lenses are not recommended unless the area used for tonal interpretation is limited to a relatively small nadir scan range.

The flight time has an impact on illumination conditions. If the solar altitude at times of repeated overflights can be kept constant, or at least within a range of about $\pm$ 10°, an additional variation is eliminated. As most natural objects exhibit asymmetric reflection characteristics it may be helpful to plan the flight time in a way to minimize change in direction of illumination. If, on the other hand, the flight lines must not change, the latter recommendations are contradictive, and the mission planner will need to decide about the trade-off between these parameters.

Let us now rewrite Equation 4 for ρ:

$$\rho = \left[\left(\exp\frac{D - Do}{\gamma}\right)\frac{f/no^2}{T_1 \cdot t \cdot \rho} - Np\right]\frac{1}{H \cdot T_a} \qquad (9)$$

As we know the camera parameters, Equation 9 can be rewritten as:

$$\rho = \left(\frac{k}{H \exp\,(Do/\gamma)} - \frac{Np}{H}\right)\frac{1}{T_a} \qquad (10)$$

where k is a constant (depending on location within frame and wavelength). The unknown parameters $1/[Hexp(Do/\gamma)]$ and Np/H are now determined by the aid of two ground truth measurements ρ_1 and ρ_2, where T_a is interpolated from Figure 8. The solution, however, is not straightforward as Np depends on nadir scan angle. If no better model is available the easiest way to obtain a solution is the fitting of a curve to three points of known reflectances. Two to three iterations are usually enough to obtain a satisfying distribution function.

CONCLUSIONS

The accuracy of the outlined correction method was tested on targets of known reflectances. The criteria for the selection of the test areas were their diffusing surfaces. The three areas showed up in three consecutive frames. Three of the total nine targets were used for the computation of the illumination parameters. Thus, six control points were left for the test of the sensitivity of the system (Table 3).

Comparing the results in Part 3.3 with the values in Part 3.1 we certainly cannot speak of any improvements. Nevertheless, both parts show one set of data of very good agreement with the true values. For Part 3.1 it is the blue band and for Part 3.3 it is

TABLE 3. REFLECTANCE VALUES

	Target	Frame No.	Dist. from p. point (mm)	ρ BLUE meas. (%)	ρ BLUE comp. (%)	ρ GREEN meas. (%)	ρ GREEN comp. (%)	ρ RED meas. (%)	ρ RED comp. (%)	ρ IR meas. (%)	ρ IR comp. (%)
Part 3.1*	Quad	1	29.1	6	6	9	44	20	11	31	17
		2	29.8	6	4	9	4	20	13	31	17
		3	50.4	6	3	9	1	20	5	31	14
	More	1	30.4	4	4	7		9	4	12	10
		2	15.0	used for the computation of parameters							
		3	34.8	4	4	7	2	9	5	12	12
	Tennis	1	26.1	14	12	21	11	22	8	45	18
		2	7.6	used for the computation of parameters							
		3	32.8	14	14	21	11	22	10	45	18
Part 3.2	Quad	1	29.1	6	8	9	12	30	26	31	29
		2	29.8	used for computation of parameters							
		3	50.4	6	5	9	7	30	33	31	36
	More	1	30.4	4	6	7	12	9	5	12	6
		2	15.0	used for computation of parameters							
		3	34.8	4	6	7	6	9	12	12	15
	Tennis	1	26.1	14	13	21	21	22	18	45	42
		2	7.6	used for computation of parameters							
		3	32.8	14	16	21	24	22	26	45	48
Part 3.3	Quad	1	29.1	6	15	9	20	20	49	31	29
		2	29.8	6	12	9	20	20	57	31	29
		3	50.4	6	32	9	38	20	25	31	36
	More	1	30.4	4	13	7	21	9	20	12	6
		2	15.0	used for computation of parameters							
		3	34.8	4	17	7	18	9	40	12	15
	Tennis	1	26.1	14	20	21	28	22	33	45	42
		2	7.6	used for computation of parameters							
		3	32.8	14	28	21	37	22	57	45	48

*Part 3.1. Reflectance values computed from measured film density without applying any corrections. Two ground measurements were used to establish the interpolation graphs for image density and object reflectance.

Part 3.2. Reflectance values corrected for camera and environmental variations.

Part 3.3. Values corrected for camera variations only (irradiance and path radiance are considered to be independent of scan angle).

the infrared band. The reason for the shift is readily found in the distribution of the path radiance. In the blue band back scattering compensates almost completely for the loss of image plane irradiance towards the edges.[1] At the same time the scattering for the longer wavelengths was of less importance on the day of overflight. The adjustment computed with the assumption of a path radiance independent of scan angle can therefore be considered as correct for the infrared band. Part 3.2 shows the results if these findings are incorporated into Equation 10.

Thus, the method for the computation of ground reflectance as it has been explained in this paper allows for measurements of an accuracy of ± 3 percent. It has been shown that the accuracy depends greatly on the knowledge of the actual path radiance distribution. Some information in this respect can be obtained by fitting an approximate function to the ground control measurements.

Without any doubt the 1^2S camera is an inexpensive sensor system. Despite its many shortcomings it is surprising what accuracy can be achieved. However, a few points should be mentioned that need special attention.

- At regular intervals the shutter performance and the flatness of the filters should be checked to maintain the reliability of the calibrated parameters.
- The author strongly recommends the use of 150-mm focal length lenses instead of the tested 100-mm lenses. The reason is mainly the smaller scan angle and, as a consequence, a reduced variation of the important parameters depending on relative position in the frame.
- The calibration of this camera system is not complete at the present stage. An important part is missing: the metric calibration. The metric calibration will determine the limit

of multiband spatial resolution for which color fidelity can be maintained. So far it has been shown that the true ground color can be computed, but the minimum resolved ground areas for which this true color is valid is unknown. Special attention has to be paid to individual distortion and aberration characteristics of the four lenses.

- The industry, or competent test labs such as the National Bureau of Standards, should calibrate systems as to important spectral parameters just as is done with metric cameras as to distortion and focal length. Only thus will consistency and reliability of measurements be effectively available to the normal user.

ACKNOWLEDGMENT

The author wishes to thankfully acknowledge the constant encouragement and personal interest of his advisor, Prof. J. E. Colcord, whose support helped to overcome some of the seemingly insolvable problems. The author also wishes to thank Dr. Jerry Vlcek, whose suggestions became fundamental to the chosen approach.

The research was sponsored by the USGS-EROS program under contract No. 14-08-0001-12865.

REFERENCES

1. Duddek, M. (1970): "Lenses and Technique for Aerial Color," *Photogrammetric Engineering*, Vol. 36, pp. 58.
2. Jensen, N. (1968): *Optical and Photographic Reconnaissance Systems*, New York, John Wiley and Sons.
3. Langford, M. J. (1969): *Advanced Photography*, London, The Focal Press.
4. Middleton, W. E. K. (1968): *Vision through the Atmosphere*, University of Toronto Press.
5. Piech, K. P. and Walker, J. E. (1971): "Aerial Color Analyses of Water Quality," *Journal of the Surveying and Mapping Division*, ASCE, Vol. 97, pp. 185.
6. Slater, P. N. and Keenan, P. B. (1969): *Preliminary Post-Flight Calibration Report on Apollo 9 Multiband Photography Experiments* SO 65, Optical Science Center, Tucson.
7. Turner, R. E. et al. (1971): "Importance of Atmospheric Scattering in Remote Sensing," *Proc. 7th Internat. Symposium on Remote Sensing of Environment*, Vol. 3, pp. 1651.
8. Turner, R. E. (1972): "Remote Sensing in Hazy Atmospheres," *Proc. 38th Annual Meeting*, American Society of Photogrammetry.
9. Yost, E. F. and Wenderoth, S. (1967): "Multispectral Color Aerial Photography," *Photogrammetric Engineering*, Vol. 33, pp. 1020.